Relation between structural disorder and fracture mechanisms in an alkali borosilicate glass : a molecular dynamics study

Le-Hai Kieu[1] Jean-Marc Delaye[1,a] Richard Caraballo[1],
Mickael Gennisson[1], Claude Stolz[2]

[1] Service d'Études et Comportement des Matériaux de Conditionnement, DEN/DTCD/SECM,
CEA Marcoule, BP 17171, 30207 Bagnols sur Cèze cedex, France

[2] Laboratoire de Mécanique des Solides, CNRS UMR7649, École Polytechnique,
91128 Palaiseau cedex, France

[a] jean-marc.delaye@cea.fr

Keywords: Molecular dynamics, Fracture, Borosilicate glass, Irradiation

Abstract. Molecular dynamics simulations were implemented to model fracturing in simplified glasses representative of actual nuclear glasses. The application of a faster thermal quenching algorithm allowed us to simulate a disordered and depolymerized structure constituting a model of a glass irradiated by deposited nuclear energy. At the same time, Vickers indentation tests were performed to measure the fracture toughness of a glass specimen of the same composition that had received a large dose of elastic energy. Numerical calculations showed an increase in the plasticity of the more rapidly quenched glass that can be attributed to a reduction in the average degree of polymerization of the glass, especially around boron atoms. The increased plasticity delays crack propagation because a larger number of plastic dislocations is required. This observation at the scale of the glass nanostructure is proposed to account for the experimentally observed fracture toughness.

Introduction

Nuclear glasses [1,2] used for the containment of long-lived radioactive waste arising from spent fuel reprocessing are intended for disposal in deep geological formations over periods of several thousand years. Over time the glass will be subjected to internal irradiation by the presence of radioactive elements, as well as to aqueous alteration. It is important to determine the fracture behavior of nuclear glasses and the influence of irradiation on crack propagation because exchanges between the glass and the environment occur via the exposed surfaces of the glass, especially cracks.

This study thus applied the method of classical molecular dynamics to elucidate the fracture mechanisms in simplified nuclear glasses subjected to external tensile stress. The effect of irradiation was taken into account indirectly by fabricating and fracturing depolymerized and disordered structures representative of glass that had received a significant elastic energy deposit [3]. These structures were obtained by accelerating the quenching rate as they were formed [4].

Experimentally, a glass specimen of the same composition as the simulated glass was subjected to $^{10}B(n,\alpha)^{7}Li$ irradiation to deposit elastic energy of the same order of magnitude as received by actual nuclear glasses. The fracture toughness of this glass was measured by Vickers nanoindentation and compared with the fracture toughness of the unirradiated glass.

Simulation method

Glass fabrication and fracturing by classical molecular dynamics. "SBN14" glass (67.7% SiO_2 – 18.1% B_2O_3 – 14.2% Na_2O) has the same molar ratios as the constituents of the actual nuclear glass.

Empirical interaction potentials were recently fitted to accurately reproduce the structures and the mechanical properties of SiO_2-B_2O_3-Na_2O glasses over a wide range of compositions [5]. These are Buckingham pair potentials with the following analytical formulation:

$$\varphi_2\left(r_{ij}\right) = \frac{q_i q_j}{r_{ij}} + B_{ij}\exp\left(-\frac{r_{ij}}{\rho_{ij}}\right) - \frac{C_{ij}}{r_{ij}^6} \quad (1)$$

where r_{ij} is the interatomic distance between atoms i and j. The first term on the right corresponds to the Coulomb energy. The q_i and q_j terms are the charges of atoms i and j, respectively. The second term represents the repulsion of atoms as their electron clouds merge. It contains two adjustable parameters depending on the nature of atoms, B_{ij} and ρ_{ij}. The last term is a dispersion term involving the adjustable parameter C_{ij} dependent on the nature of the interacting atoms.
The parameter fitting method was detailed at length in reference [5]. To obtain a better representation of the glass structural and mechanical properties over a wide composition range, we added a dependence between the ion charge and the glass composition. This dependence is important to accurately reproduce the nonlinearities associated with the boron anomaly [6,7]. The ionic charges used for simulation of SBN14 glass are indicated in Table 1. The calculations were performed with the DL_POLY3 code [8].

Table 1**.** Charge values for simulation of SBN14 glass

	q_{Si}	q_B	q_{Na}	q_O
SBN14 glass	1.868	1.599	0.450	−0.967

SBN14 glass was prepared as follows. Initially, a liquid comprising 100 000 atoms was equilibrated at 5000 K for 100 ps. The time step was 1 fs. The initial glass density was chosen lower than the experimental density to take into account the glass contraction during cooling. The liquid structure was quenched at a rate of 5×10^{12} K/s while maintaining a constant volume; the temperature was lowered in 100 K steps from 5000 K to room temperature. The resulting solid structure was relaxed for 20 ps in the NPT ensemble at room temperature with zero external pressure to determine its equilibrium volume. The final glass relaxation was obtained in the NVE ensemble by maintaining the volume equal to the previously determined equilibrium volume; this step lasted 5 ps.
Born-von Karman periodic boundary conditions were applied along the three directions during the glass preparation. The full Ewald sum [9] with 10^{-5} precision was used for the Coulomb interactions.
The simulation cells containing the glassy structures were fractured as follows. Atoms were first removed in order to notch one face of the simulation cell as shown in Figure 1. The notch was 30 Å deep and 20 Å high. The notched samples were relaxed at 5 K for 50 ps before being fractured.

Periodic boundary conditions are applied on the X and Y axes but are eliminated along the vertical Z axis to allow the application of the tensile stress. To avoid surface effects following the elimination of periodic conditions on the Z axis, two layers are frozen at the top and bottom of the simulation cell. In these layers, which are 11.5 Å thick (slightly greater than the potential cutoff radius), the atom positions are fixed and do not conform to the equations of motion of classical molecular dynamics.
To fracture the samples a tensile force is applied by imposing progressive displacements in the Z direction on the atoms of the frozen layers. A displacement is applied at each time step with a strain rate of 4×10^{-6} fs^{-1}. The temperature is maintained at 5 K throughout the duration of fracturing to avoid adding thermal effects to the tensile effects.

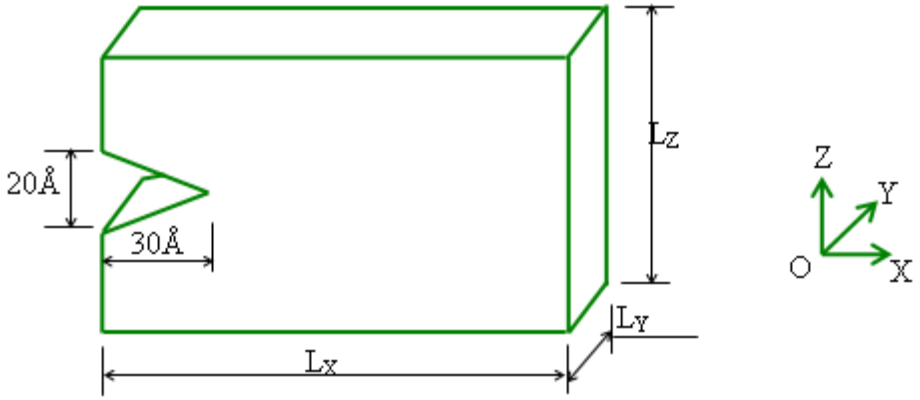

Fig. 1. Glass sample before fracturing

Preparation of glass specimen representative of irradiated glass. As it was not possible to completely irradiate the glass samples by displacement cascades [3,10] for reasons of computation time, we adopted a method based on accelerating the quenching rate. This technique produced glass with lower density than before, and with a lower degree of polymerization and a greater degree of disorder. The effect of the accumulation of displacement cascades was thus qualitatively reproduced [3]. The glass disordered and depolymerized by acceleration of the quenching rate is considered a model for glass irradiated by deposited elastic energy.

Experimental fracture toughness measurement. SBN14 glass specimens were irradiated by $^{10}B(n,\alpha)^{7}Li$ reaction of a neutron flux in the Osiris reactor [11]. The total ballistic energy received by the glass was estimated at 2.38 dpa with the SRIM code. The fracture toughness of the pristine glass and irradiated glass was measured by Vickers indentation with loads ranging from 75 g to 400 g. For a given load, if the size of the indentation is characterized by a diagonal *d*, the hardness *H* is measured by the formula:

$$H = \frac{1.854F}{d^2} \tag{2}$$

where *F* is the force applied and *d* is the length of the indentation diagonal. When cracks appear at the corners of the indentation, the mean crack length *c* is measured with an optical microscope and the fracture toughness is calculated [[12]**Ошибка! Источник ссылки не найден.**]:

$$K_{IC} = 0.057H\sqrt{a}\left(\frac{E}{H}\right)^{2/5}\left(\frac{c}{a}\right)^{-3/2} \tag{3}$$

where *a* is the half-length of the indentation diagonal, and *E* is Young's modulus.
The fracture toughness of unirradiated SBN14 glass was measured by averaging the values obtained for 25 indentations (for loads between 75 g and 200 g): 0.76 ± 0.06 MPa·m$^{1/2}$. The fracture toughness of irradiated SBN14 glass was determined by averaging the values obtained for 20 indentations (for loads between 200 g and 400 g): 0.88 ± 0.06 MPa·m$^{1/2}$.

Fracturing of SBN14 glass by classical molecular dynamics

Stress/strain curves. The stress/strain curve to failure is plotted in Figure 2 for the initial and fast-quenched SBN14 glass specimens. The stress/strain curves exhibit a classic shape[[13]**Ошибка!**

Источник ссылки не найден.], with a linear stress increase versus strain for small (elastic) deformations, followed by a plateau in which the stress varies little while the strain continues to increase, and a decreasing leg where the stress diminishes to structural decohesion. The last two stages correspond to plastic deformation of the structure.

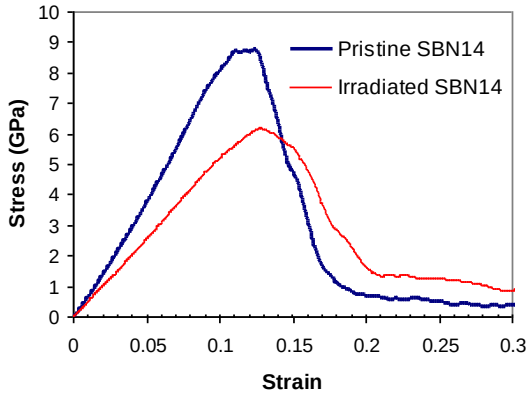

Fig. 2. Stress/strain curves for fracturing of initial and fast-quenched SBN14 glass specimens

Young's modulus was estimated from the slope of the initial linear portion of the stress/strain curve. Young's modulus for the initial glass was 74.0 GPa, relatively near the experimental value of 82 GPa. At atomistic scale the fracturing of simulation cells comprises four phases: nucleation of cavities, growth of cavities, coalescence of cavities, then decohesion. Cavity nucleation begins during the elastic deformation phase and continues during the plastic deformation phase, while cavity growth corresponds to the plastic deformation phase. Coalescence and decohesion occur during the sudden drop in the stress level.

Atomistic mechanisms responsible for fracturing. To analyze the structural changes that accompany glass fracturing, the radial distribution functions of the Si-O and B-O pairs were plotted at different moments.

The evolution of the Si-O radial distribution functions is shown in Figure 3. Only the first peak of the function is indicated, as the subsequent peaks do not show any significant changes.

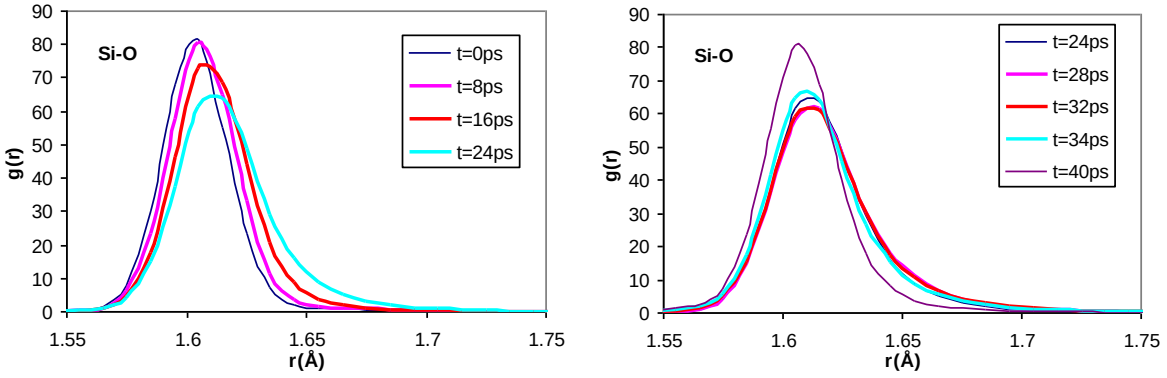

Fig. 3. Si-O radial distribution functions at different moments during fracturing

Figure 3 is separated into two parts for clarity. In Figure 3a, between 0 ps and 24 ps, the maximum peak value can be seen to decrease and shift toward greater radii. This indicates stretching of the Si-O bonds together with increasing structural tension. Coalescence and decohesion of the structure occur between 24 ps and 40 ps. The Si-O radial distribution function gradually recovers its initial shape. The growth and subsequent coalescence of cavities creates new free surfaces within the structure, relieving the local stresses responsible for the deformation of the Si-O bonds.
The B-O radial distribution functions are plotted in Figure 4. Only the first peak of the functions is shown in the figure; the subsequent peaks do not show any significant changes. The distances between tricoordinate boron and oxygen atoms are shorter on average than the distances between tetracoordinate boron and oxygen, which explains the existence of two sub-peaks. The peaks are distinctly separated because the calculations were performed at low temperatures.

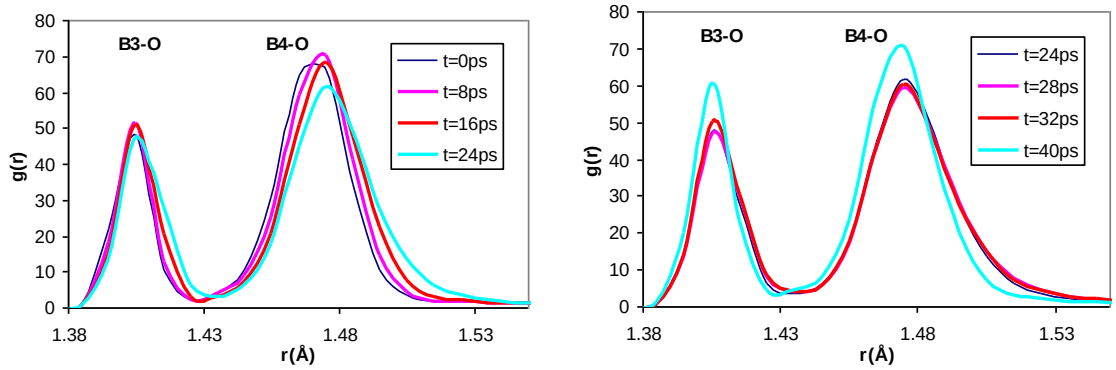

Fig. 4. B-O radial distribution functions at different moments during fracturing.

A difference is visible in the behavior of B-O bonds depending on the boron coordination number. The $^{[4]}$B-O bonds behave qualitatively like Si-O bonds: they stretch initially because of the local tensile stress application, then return to their original state following the creation of new free surfaces during the cavity coalescence.
The $^{[3]}$B-O bonds behave differently. No significant stretching appears between 0 and 40 ps. The height of the first maximum of the peak corresponding to the $^{[3]}$B-O bonds at the end of fracture is simply observed to increase, reflecting an increase in the concentration of tricoordinate boron atoms compared with tetracoordinate boron.
The environments of tricoordinate boron atoms are thus less deformed than the environments of tetracoordinate boron atoms. The following explanation is proposed: the local degrees of freedom are greater around BO_3 entities because of smaller the number of chemical bonds that bind them to the polymerized network. They are free to reorient themselves, and can thus adapt more readily to external stresses.

Effect of fast quenching

The same approach was applied to the fast-quenched glass. The stress/strain curve is shown in Figure 2. As a result of fast quenching, a reduction of about 30% is observed for the initial slope corresponding to Young's modulus (Young's modulus was 51.6 GPa for the fast-quenched glass), as well as a lengthening of the duration of the plastic phase. The cavities formed are systematically more numerous in the fast-quenched glass, which contains a larger free volume fraction that facilitates cavity nucleation. At a structural level, fast quenching increases the concentration of 3-coordinate boron atoms to the detriment of 4-coordinate boron atoms. This phenomenon explains why plastic deformation processes are more numerous in the fast-quenched glass, because tricoordinate boron atoms are involved in plastic flow.

Comparison with experimental findings

The simulation shows an increase in plastic deformation in the rapidly quenched glass specimens combined with a decrease in the $^{[4]}B/^{[3]}B$ ratio. This results in delayed fracturing.

Experimentally, Vickers indentation measurements showed increased fracture toughness of the glass after being subjected to a large number of atomic displacements by deposition of elastic energy. Comparing these results suggests an explanation for the increase in fracture toughness under irradiation. The average degree of polymerization diminishes in glass subjected to elastic energy deposition, thereby increasing its plasticity by facilitating local reorganization. Ultimately the energy required to propagate a fracture in the glass increases, which explains the greater fracture toughness.

Conclusion

Molecular dynamics simulations were implemented to model fracturing in simplified glasses representative of actual nuclear glasses. The application of a faster thermal quenching algorithm allowed us to simulate a disordered and depolymerized structure constituting a model of a glass irradiated by deposited nuclear energy. At the same time, Vickers indentation tests were performed to measure the fracture toughness of a glass specimen of the same composition that had received a large dose of elastic energy.

Numerical calculations showed an increase in the plasticity of the more rapidly quenched glass that can be attributed to a reduction in the average degree of polymerization of the glass, especially around boron atoms. The increased plasticity delays crack propagation because of the larger number of plastic deformations required. This observation at the scale of the glass nanostructure is proposed to account for the experimentally observed fracture toughness.

References

[1] S. Peuget, P.-Y. Noël, J.-L. Loubet, S. Pavan, P. Nivet, A. Chenet, Nucl. Instr. and Meth. B Vol. 246 (2006) p. 379

[2] W.J. Weber, R.C. Ewing, C.A. Angell, G.W. Arnold, A.N. Cormack, J.M. Delaye, D.L Griscom, L.W. Hobbs, A. Navrotsky, D.L. Price, A.M. Stoneham, M.C. Weinberg, J. Mater. Res. Vol. 12 (1997) p.1946

[3] J.-M. Delaye, G. Bureau, S. Peuget, G. Calas, J. Non-Cryst. Solids Vol. 357 (2011) p. 2763

[4] S. Ito, T. Taniguchi, J. Non-Cryst. Solids Vol. 349 (2004) p. 173

[5] L.-H. Kieu, J.-M. Delaye, L. Cormier, C. Stolz, J. Non-Cryst. Solids, Vol. 357 (2011) p. 3313

[6] Y.H. Yun, P.J. Bray, J. Non-Cryst. Solids Vol. 27 (1978) p. 363

[7] D. Manara, A. Grandjean, D.R. Neuville, J. Non-Cryst. Solids Vol. 355 (2009) p. 2528

[8] Information on http://www.stfc.ac.uk/CSE/os/25526.aspx

[9] S. Deleeuw, J.W. Perram, E.R. Smith, Proc. R. Soc. London A Vol. 373 (1980) p. 27

[10] J.-M. Delaye, D. Ghaleb, Phys. Rev. B Vol. 71 (2005) p. 224204

[11] T. Fares, PhD Thesis, University of Montpellier II (2011)

[12] Hj. Matzke "CEA/Valrhô Summer Session Proceedings on Glass : Scientific Research for High Performance Containment", Méjannes-Le-Clap (1997), p. 149

[13] T.P. Swiler, T. Varghese, J.H. Simmons, J. Non-Cryst. Solids Vol. 181 (1995) p. 238